

Decoration of reduced graphene oxide with polyaniline film and their enhanced microwave absorption properties

Panbo Liu · Ying Huang

Received: 26 November 2013 / Accepted: 31 March 2014 / Published online: 9 April 2014
© Springer Science+Business Media Dordrecht 2014

Abstract The composites of reduced graphene oxide-polyaniline film (RGO-PANI) were synthesized by an in situ polymerization method and the microwave absorption properties of the composites were investigated. FESEM results indicate that RGO is covered with polyaniline film, and some PANI nanoparticles with the diameter in the range of 10–30 nm embed in the film. As PANI film covered on RGO, the microwave adsorption properties of RGO are significantly enhanced. The maximum reflection loss of RGO-PANI is up to -41.4 dB at 13.8 GHz and the bandwidths exceeding -10 and -20 dB are 4.2 GHz (from 11.7 to 15.9 GHz) and 1.5 GHz (from 12.8 to 14.3 GHz) with a coating layer thickness of 2 mm. The excellent microwave absorption properties of the composites may be attributed to the unique structural characteristics and the charge transfer between RGO and PANI film. Thus, the composites can be used as an attractive candidate for the new type of microwave absorption materials.

Keywords Graphene · Polyaniline nanoparticles · Dielectrics · Microwave absorption properties

Introduction

Microwave absorption materials can absorb electromagnetic (EM) waves effectively and convert EM energy into thermal energy or dissipate the EM waves by interference. Most of the microwave absorbers are composed of magnetic loss powders [1, 2], dielectric loss materials [3] or conducting polymers [4].

However, the attenuation mechanism of those materials is mainly based on either dielectric loss or magnetic loss.

Carbon based materials with low density and high complex permittivity can be used as lightweight microwave absorption materials. Reduced graphene oxide (RGO), a new kind of carbon based material, has attracted tremendous scientific attention in recent years due to its unique physical, chemical and mechanical properties [5, 6]. Wang [7] studied the microwave absorption property of RGO and concluded that the value of microwave absorption is -6.9 dB, which was not an ideal microwave absorption material. Polyaniline (PANI), one of the most promising conductive polymers, has high electrical conductivity and excellent environmental stability and can be used as microwave absorption materials. However, high complex permittivity and low complex permeability usually present difficulties in impedance matching, resulting in weak microwave absorption [8]. Recently, some magnetic particles have been added into PANI to enhance the microwave absorption properties [9–11]. It is well-known that the crystal structure, size and special geometrical morphology of the microwave absorbers may have an important influence on the permittivity and permeability [12]. In recent progress, the microwave absorption properties of PANI could be effectively adjusted by their morphology and structure even in the absence of any magnetic particles [13, 14]. Oyharçabal [15] studied the influence of PANI morphology on the microwave absorption properties and find that flake-like PANI can improve the microwave absorption properties. Zhang [16] synthesized a series of PANI materials by a reverse dropping method and discussed the microwave absorption of PANI nanoparticles. The results indicate that PANI nanoparticles have a reflection loss of -40.5 dB at 5.8 GHz and the excellent microwave absorption abilities is due to their distinguishable physical properties. Yu [17] reported an in-situ polymerization process to synthesize graphene/polyaniline nanorod arrays, and the maximum reflection loss is -45.1 dB with a thickness

P. Liu · Y. Huang (✉)

Key Laboratory of Space Applied Physics and Chemistry, Ministry of Education, School of Science, Northwestern Polytechnical University, Xi'an 710129, People's Republic of China
e-mail: yingh@nwpu.edu.cn

of 2.5 mm. Although many research workers have been focused on the microwave absorption properties of PANI, up to now, the microwave absorption properties of PANI film covered on the surface of RGO have never been reported.

In this work, we report an in situ polymerization process to synthesize RGO-PANI and investigate the microwave absorption properties. As PANI film covered on RGO, the microwave absorption properties of the composites are significantly enhanced. The results indicate that the maximum reflection loss of RGO-PANI is -41.4 dB and the bandwidths exceeding -10 and -20 dB are 4.2 and 1.5 GHz, respectively, with a thickness of 2 mm. The composites are very promising as a possible candidate for the new microwave absorption materials.

Experimental

Graphene oxide (GO) was synthesized by Hummers method [18]. The RGO-PANI composites were synthesized as follows: 0.1 g of GO was dispersed in 100 mL distilled water and ultrasonicated for 2 h until GO was fully dispersed. Afterward, 0.1 mL of aniline monomer and 4 mL of concentrated H_2SO_4 were added into the above solution and stirred for 30 min at 0 °C to form a uniform mixture. The oxidant, ammonium persulfate dissolved in distilled water, was added into the solution and the mixture was stirred for 24 h at 0 °C. The product was washed with distilled water. 0.1 mL hydrazine monohydrate was added to the above suspension and heated to 90 °C for 24 h. The obtained product was washed with water and dried in a vacuum oven at 60 °C.

The FT-IR spectra were observed by iS10 (USA). XRD were identified by X-ray powder diffraction (XRD, Philips X-ray diffractometer, PW3040). X-ray photoelectron spectroscopy (XPS, Thermal Scientific K Alpha) was performed with a Phoibos 100 spectrometer. Raman scattering was performed on a Jobin-Yvon HR800 Raman spectrometer. The morphology was observed by field emission scanning electron microscope (FESEM: Quanta 600FEG). Thermal gravimetric (TG) analysis was performed on a Q2000 thermogravimetric analyzer at a heating rate of 10 °Cmin $^{-1}$ in air. For measurement of the microwave properties, the samples were dispersed in paraffin homogeneously with a sample-to-paraffin volume ratio of 1:1, and then the mixture was pressed into a toroidal shape with an inner diameter of 3.0 mm and an outer diameter of 7.0 mm. The relative complex permittivity (ϵ' and ϵ'') and permeability (μ' and μ'') were carried out by a HP8753D vector network analyzer at the frequency range of 2–18 GHz.

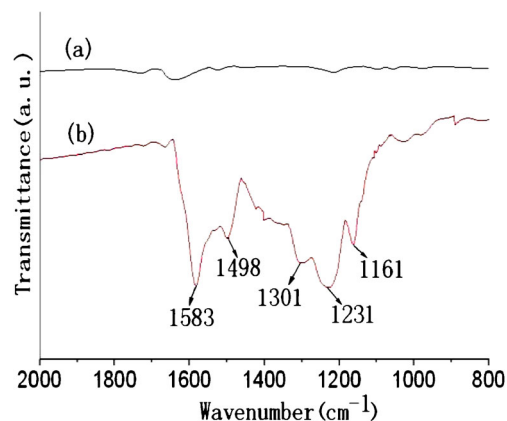


Fig. 1 FT-IR spectra of RGO (a) and RGO-PANI (b)

Results and discussion

FT-IR spectrum of RGO and RGO-PANI are presented in Fig. 1. In Fig. 1a, the featureless spectra indicates that GO is reduced to RGO successfully [19]. For RGO-PANI in Fig. 1b, the characteristic bands at $1,583$ and $1,497$ cm^{-1} are ascribed to the stretching vibration of $C=N$ and $C=C$ stretching of the quinonoid and benzenoid units [20], respectively. The peak at $1,301$ cm^{-1} is attributed to the $C-N$ stretching of the secondary aromatic amine. The peak at $1,231$ cm^{-1} is due to the $C-N^+$ stretching and the peak at $1,126$ cm^{-1} is assigned to the stretching vibration of $=N^+$ in the bipolaron form of PANI emeraldine salt, respectively [21]. The presence of these peaks clearly suggests the formation of PANI in the composites.

The phase structure of the as-synthesized samples is determined by XRD in Fig. 2. In Fig. 2a, it can be observed that RGO exhibits a diffraction peak at $2\theta=24.6^\circ$, which can be attributed to the graphitic structure (002) of short-range order in stacked RGO [22]. For RGO-PANI (Fig. 2b), the crystalline peaks appear at $2\theta=15.3^\circ$, 19.8° and 25.4° corresponding to the (011), (020) and (200) crystal planes of PANI in its emeraldine salt form, indicating that RGO are completely covered by PANI [23]. The diffraction peak of RGO in the

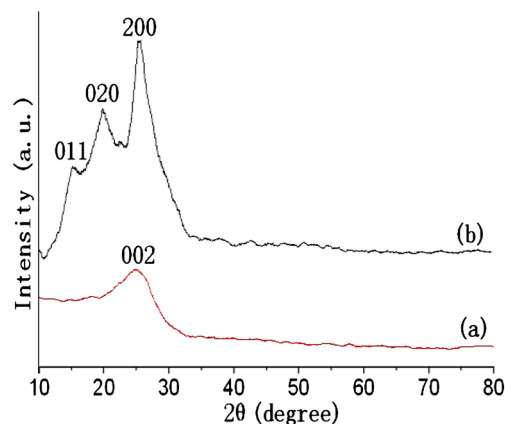


Fig. 2 XRD patterns of RGO (a) and RGO-PANI (b)

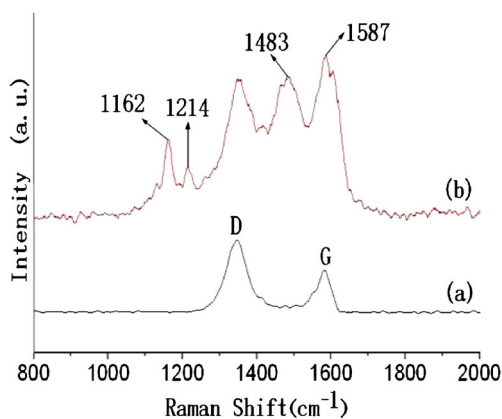


Fig. 3 Raman spectra of RGO (a) and RGO-PANI (b)

composites is not observed in the composites, which is due to the poor crystalline nature [24].

Figure 3 shows the Raman spectra of RGO and RGO-PANI. In Fig. 3a, it can be seen that RGO exhibits two typical bands, the D band at $1,347\text{ cm}^{-1}$ is assigned to the vibrations of sp^3 carbon atoms of disordered graphite and the G band at $1,581\text{ cm}^{-1}$ is mainly assigned to the in-plane vibration of sp^2 carbon atoms in a 2D hexagonal lattice [25]. As for RGO-PANI in Fig. 3b, the bands at $1,162$, $1,214$, $1,483$ and $1,587\text{ cm}^{-1}$ can be assigned to in plane C-H bending of quinoid, C-N stretching vibrations, C=N stretching, and C=C stretching vibration, respectively, indicating the presence of doped PANI structure on the surface of RGO [26, 27]. In addition, the D and G bands in RGO-PANI exhibit a blue shift compared with that of RGO, the D band shifts from $1,347$ to $1,354\text{ cm}^{-1}$, whereas the G band varies from $1,581$ to

$1,602\text{ cm}^{-1}$. The respective blue shift between PANI film and RGO is due to the strong interaction between the two components [28].

The elemental components of the RGO-PANI composites are further investigated by XPS in Fig. 4. In Fig. 4a, the C1s spectrum of GO can be deconvoluted into four different peaks. The peaks at 284.6, 286.4, 287.8, and 289.3 eV have been assigned to the C-C/C=C in the aromatic rings, C-O of epoxy and/or alkoxy, C=O and O-O=O groups, respectively [29]. As for RGO-PANI in Fig. 4b, the intensities of the carbon binding to oxygen, especially the peak of C-O, decrease dramatically, revealing that most of the oxygen-containing functional groups have been removed. Meanwhile, a new peak at 285.6 eV can be assigned to the C-N bond of PANI [30]. In Fig. 4c, the wide scan XPS spectrum indicates that the composites are completely composed of C, N and O elements. No other elemental signals are detected in the general XPS spectrum. In Fig. 4d, N 1s XPS spectra of RGO-PANI can be deconvoluted into three components, the peak at 398.2 eV is attributed to the quinoid imine (=N-), the peak at 399.0 eV is related to the benzenoid amine (-NH-) and the peak at 400.4 eV is assigned to the cationic nitrogen atoms (N^+), respectively [31]. The appearance of the above peaks suggests the formation of doped PANI.

The microstructure and detailed morphology of RGO-PANI have been examined by FESEM and the results are presented in Fig. 5. In Fig. 5a, it can be found that the surface of RGO is covered with polyaniline film, and many protuberances are the homogeneous PANI nanoparticles. From the bent and flat morphology, we can observe that the composites

Fig. 4 C1s XPS spectra of GO (a) and RGO-PANI (b), survey scan (c) and N1s XPS spectra (d) of RGO-PANI

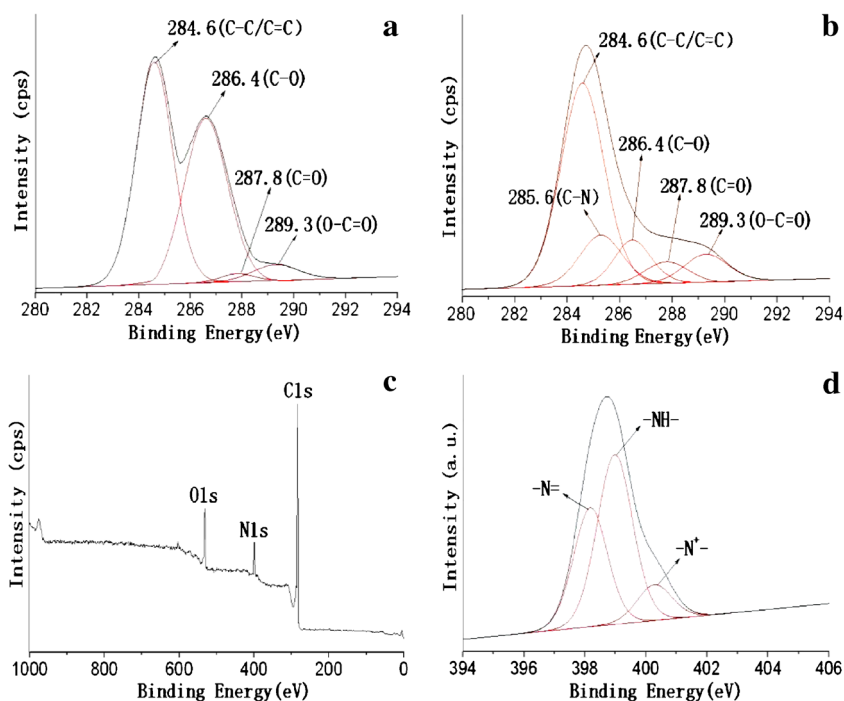


Fig. 5 FESEM images of RGO-PANI

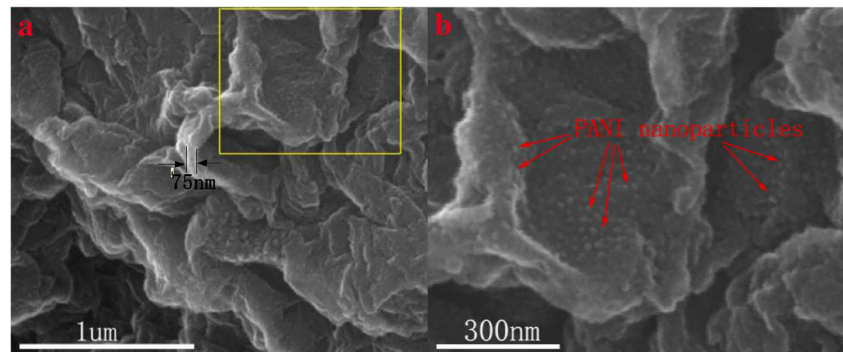


exhibit flexible character and the good mechanical performances are due to the introduction of RGO. At the same time, no free PANI film or naked RGO sheets are observed, indicating that the nucleation and growth of PANI film only occur on the surface of RGO. Furthermore, the composites show a free-standing sheet-like morphology with a thickness of 75 nm. Fig. 5b shows the enlarged images of RGO-PANI (yellow regions), respectively. It can be clearly observed that a large quantity of PANI nanoparticles with a relatively uniform size compactly embed in the film and the diameter of PANI nanoparticles are in the range of 10–30 nm, as indicated by the red arrows. This may be favorable for the enhancement of the charge transfer between RGO and PANI film, which can be used as excellent microwave absorbers.

To understand the possible microwave absorption mechanisms, the complex permittivity real part (ϵ'), permittivity imaginary part (ϵ''), permeability real part (μ'), permeability imaginary part (μ''), dielectric loss tangent ($\tan\delta\epsilon$) and magnetic loss tangent ($\tan\delta\mu$) of RGO-PANI are investigated in Fig. 6. In Fig. 6a, it can be observed that ϵ' values vary from

14.5 to 7.3 and ϵ'' values decrease from 9.8 to 1.1 with several fluctuations in the frequency range of 2–18 GHz. In Fig. 6b, it reveals that the values of μ' are in the range of 0.8–1.0 and the μ'' values are less than 0.28 over 2–18 GHz. The dielectric loss tangent ($\tan\delta\epsilon$) and magnetic loss tangent ($\tan\delta\mu$) of RGO-PANI are shown in Fig. 6c, it can be noted that the values of $\tan\delta\epsilon$ are higher than $\tan\delta\mu$ in frequencies ranging from 2 to 18 GHz, suggesting that the composites is mainly dependent on the dielectric loss.

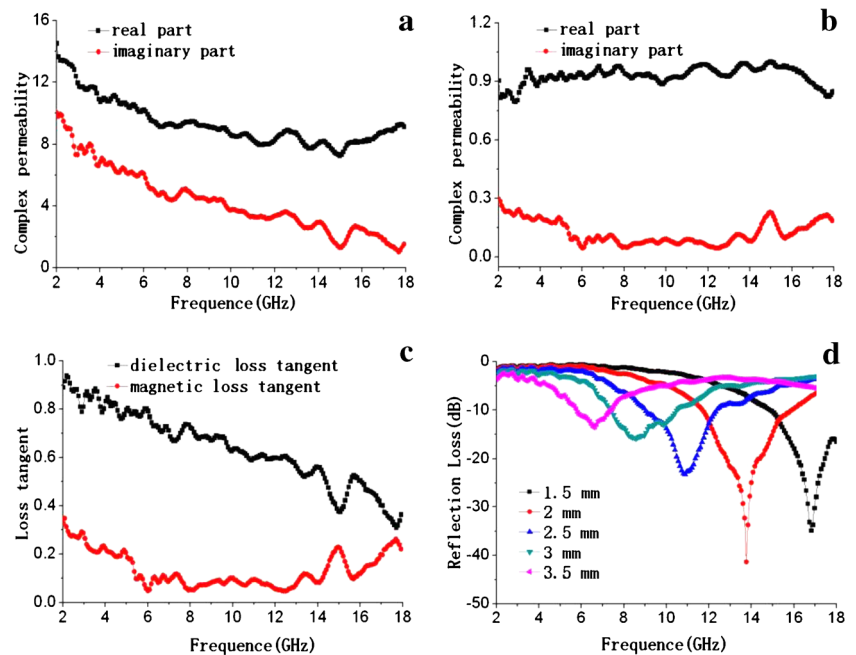
To clarify the EM absorption properties, the reflection losses (R_L) are calculated according to

$$R_L(\text{dB}) = 20 \log \left| \frac{Z_{in} - 1}{Z_{in} + 1} \right| \quad (1)$$

$$Z_{in} = \sqrt{\mu_r / \epsilon_r} \tanh [j(2\pi f d / c) \sqrt{\epsilon_r \mu_r}] \quad (2)$$

Where Z_{in} is the input impedance of the absorber, c is the velocity of electromagnetic waves in free space, f is the frequency, and d is the layer thickness. In Fig. 6d, it can be

Fig. 6 Frequency dependence of the complex relative dielectric permittivity (a), the complex relative magnetic permeability (b), the loss tangent (c) and the reflection loss (d) of RGO-PANI



found that there is one sharp and strong wave absorption peak at 13.8 GHz, the maximum R_L is up to -41.4 dB and the bandwidths corresponding to the R_L values below -10 dB (90 % of EM wave absorption) and -20 dB (99 % of EM wave absorption) are 4.2 GHz (from 11.7 to 15.9 GHz) and 1.5 GHz (from 12.8 to 14.3 GHz), respectively, with a coating layer thickness of 2 mm, the calculated results demonstrate that the as-synthesized RGO-PANI composites present a better microwave absorption performance than single RGO [7], PANI [15, 16] and PANI composites [32–34]. It is well known that the composites structure, size and special geometrical morphology have an important influence on the microwave absorption [35]. Therefore, in our case, the enhanced electromagnetic absorption properties of RGO-PANI may be attributed to the unique structural characteristics and the charge transfer between RGO and PANI film. In addition, the maximum R_L values obviously shift to a lower frequency range with increasing the layer thickness. When the coating layer thickness goes up to 2.5 mm, the bandwidths of the R_L values below -10 dB are 3.4 GHz in the range of 9.0–12.4 GHz and the minimum R_L is 23.1 dB at 10.9 GHz. All of the above analyses apparently demonstrate that the composites obtained in this work are attractive candidates for the new type of EM wave absorption materials.

Conclusions

In summary, PANI film covered on the surface of RGO is successfully prepared by an in situ polymerization process. FE-SEM results show that lots of PANI nanoparticles embed in the film and the diameter of PANI nanoparticles is in the range of 10–30 nm. As PANI film anchored on the surface of RGO, the electromagnetic absorption properties are significantly enhanced. The maximum reflection loss of RGO-PANI is -41.4 dB and the bandwidths corresponding to the R_L values below -10 and -20 dB are 4.2 and 1.5 GHz, respectively, with a coating layer thickness of 2 mm. Take the above analysis, it can be summarized that RGO-PANI can be used as EM absorption materials with good absorption properties.

Acknowledgments This work was supported by the Spaceflight Foundation of the People's Republic of China (NBXW0001), the Spaceflight Innovation Foundation of China (NBXT0002) and the Doctorate Foundation of Northwestern Polytechnical University (CX201328).

References

- Li XA, Zhang B, Ju CH, Han XJ, Du YC, Xu P (2011) *J Phys Chem C* 115:12350–12357
- Gu X, Zhu WM, Jia CJ, Zhao R, Schmidt W, Wang YQ (2011) *Chem Commun* 47:5337–5339
- Gupta TK, Singh BP, Teotia S, Katyal V, Dhakate SR, Mathur RB (2013) *J Polym Res* 20:169
- Ni XW, Hu XJ, Zhou SY, Sun CH, Bai XX, Chen P (2011) *Polym Adv Technol* 22:532–537
- Novoselov KS, Geim AK, Morozov SV, Jiang D, Zhang Y, Dubonos SV, Grigorieva IV, Firsov AA (2004) *Science* 306:666–669
- Deshmukh K, Khatake SM, Joshi GM (2013) *J Polym Res* 20:286
- Wang C, Han XJ, Xu P, Zhang XL, Du YC, Hu SR, Wang JY, Wang XH (2011) *Appl Phys Lett* 98:072906
- Hosseini SH, Mohseni SH, Asadnaci A, Kerdari H (2011) *J Alloys Compd* 509:4682–4687
- Zhang B, Du YC, Zhang P, Zhao HT, Kang LL, Han XJ, Xu P (2013) *J Appl Polym Sci*. doi:10.1002/app.39332
- Belaabed B, Wojkiewicz JL, Lamouri S, Kamchi NE, Lasri T (2012) *J Alloys Compd* 527:137–144
- Gandhi N, Singh K, Ohlan A, Singh DP, Dhawan SK (2011) *Compos Sci Technol* 71:1754–1760
- Sun GB, Dong BX, Cao MH, Wei BQ, Hu CW (2011) *Chem Mater* 23:1587–1593
- Zhang X, Zhu JH, Haldolaarachchige N, Ryu J, Young DP, Wei SY, Guo ZH (2012) *Polymer* 53:2109–2120
- Lee BM, Kim JE, Fang FF, Choi HJ, Feller JF (2011) *Macromol Chem Phys* 212:2300–2307
- Oyharçabal M, Olinga T, Foulc MP, Lacomme S, Gontier E, Vigneras V (2013) *Compos Sci Technol* 74:107–112
- Zhang P, Han XJ, Kang LL, Qiang R, Liu WW, Du YC (2013) *RSC Adv* 3:12694–12701
- Yu HL, Wang TS, Wen B, Lu MM, Xu Z, Zhu CL, Chen YJ, Xue XY, Sun CW, Cao MS (2012) *J Mater Chem* 22:21679–21685
- Hummers WS, Offeman RE (1958) *J Am Chem Soc* 80:1339
- Bose S, Kuila T, Mishra AK, Kim NH, Lee JH (2012) *J Mater Chem* 22:9696–9703
- Murugan AV, Muraliganth T, Manthiram A (2009) *Chem Mater* 21:5004–5006
- Yin JB, Wang XX, Chang RT, Zhao XP (2012) *Soft Matter* 8:294–297
- Si YC, Samulski ET (2008) *Chem Mater* 20:6792–6797
- Yan J, Wei T, Shao B, Fan ZJ, Qian WZ, Zhang ML, Wei F (2010) *Carbon* 48:487–493
- Chen YJ, Wang QS, Zhu CL, Gao P, Ouyang QY, Wang TS, Ma Y, Sun CW (2012) *J Mater Chem* 22:5924–5927
- Jin Z, Yao J, Kittrell C, Tour JM (2011) *ACS Nano* 5:4112–4117
- Wang HL, Hao QL, Yang XJ, Lu LD, Wang X (2010) *Nanoscale* 2:2164–2170
- Chen F, Liu P, Zhao QQ (2012) *Electrochim Acta* 76:62–68
- An JW, Liu JH, Zhou YC, Zhao HF, Ma YX, Li ML, Yu M, Li SM (2012) *J Phys Chem C* 116:19699–19708
- Shin HJ, Kim KK, Benayad A, Yoon SM, Park HK, Jung IS, Jin MH, Jeong HK, Kim JM, Choi JY, Lee YH (2009) *Adv Funct Mater* 19:1987–1992
- Wang HL, Hao QL, Yang XJ, Lu LD, Wang X (2010) *ACS Appl Mater Interfaces* 2:821–828
- Wang HH, Zhu EW, Yang JZ, Zhou PP, Sun DP, Tang WH (2012) *J Phys Chem C* 116:13013–13019
- Li QL, Zhang CR, Li JQ (2010) *Appl Surf Sci* 257:944–948
- Ting TH, Jau YN, Yu RP (2012) *Appl Surf Sci* 258:3184–3190
- Wang Y, Huang Y, Wang QF, He Q, Chen L (2012) *Appl Surf Sci* 259:486–493
- Sun GB, Zhang XQ, Cao MH, Wei BQ, Hu CW (2009) *J Phys Chem C* 113:6948–6954